ADVANCED MATERIALS

www.advmat.de

High-Performance All-Polymer Solar Cells Enabled by an n-Type Polymer Based on a Fluorinated Imide-Functionalized Arene

*Huiliang Sun, Yumin Tang, Chang Woo Koh, Shaohua Ling, Ruizhi Wang, Kun Yang, Jianwei Yu, Yongqiang Shi, Yingfeng Wang, Han Young Woo, and Xugang Guo**

A novel imide-functionalized arene, di(fluorothienyl)thienothiophene diimide (f-FBTI2), featuring a fused backbone functionalized with electron-withdrawing F atoms, is designed, and the synthetic challenges associated with highly electron-deficient fluorinated imide are overcome. The incorporation of f-FBTI2 into polymer affords a high-performance n-type semiconductor f-FBTI2-T, which shows a reduced bandgap and lower-lying lowest unoccupied molecular orbital (LUMO) energy level than the polymer analog without F or with F-functionalization on the donor moiety. These optoelectronic properties reflect the distinctive advantages of fluorination of electron-deficient acceptors, yielding "stronger acceptors," which are desirable for n-type polymers. When used as a polymer acceptor in all-polymer solar cells, an excellent power conversion efficiency of 8.1% is achieved without any solvent additive or thermal treatment, which is the highest value reported for all-polymer solar cells except well-studied naphthalene diimide and perylene diimide-based n-type polymers. In addition, the solar cells show an energy loss of 0.53 eV, the smallest value reported to date for all-polymer solar cells with efficiency > 8%. These results demonstrate that fluorination of imide-functionalized arenes offers an effective approach for developing new electron-deficient building blocks with improved optoelectronic properties, and the emergence of f-FBTI2 will change the scenario in terms of developing n-type polymers for high-performance all-polymer solar cells.

Among various types of organic solar cells (OSCs), all-polymer solar cells (all-PSCs) consisting of a p-type polymer donor and an n-type polymer acceptor show pronounced advantages, including excellent mechanical flexibility/stretchability and improved device stability.[1] However, the power conversion efficiencies (PCEs) of all-PSCs still lagged behind those of OSCs based on fullerenes or nonfullerene small molecule acceptors.[2] To date, very few n-type polymer acceptors can yield all-PSCs with PCEs > 8% (Table S22, Supporting Information).[1e,g,3] Development of high-performance n-type polymers relies on the invention of new electron-deficient building blocks with good solubilizing capability, optimized molecular geometry, and improved electronic property.[4] They are dominated by two historical molecules till today, naphthalene diimide (NDI) and perylene diimide (PDI, **Figure 1**), which were originally used as colorants in the industry of dyes and pigments. The search for high-performance organic semiconductors has led to the resurgence of NDIs and PDIs in organic electronics field, and their incorporations into polymers have greatly improved the n-type performance of polymeric semiconductors.[4a,5] Despite of their remarkable successes, the NDI or PDI cores are hard to modify and functionalize, and the state-of-the-art polymer acceptors based on NDI and PDI suffer from a poor absorption coefficient in films due to their twisted backbones, which limits the photocurrent and efficiency improvement.[1a,g]

Invention of new electron-deficient arene with excellent solubility and optimized geometry and electronic property should offer a new paradigm for developing n-type polymers. Among various electron-deficient building blocks, bithiophene imide (BTI), as an imide-functionalized arene, has been proved as a prominent one for constructing n-type polymer semiconductors.[6] The β-positions of thiophenes in BTI afford an unprecedented opportunity for structural optimization via backbone expansion and core modification. A new generation of ladder-type BTI derivatives, BTIn, were developed recently via a ring fusion strategy,[7] which have greatly broadened the

Dr. H. Sun, Y. Tang, S. Ling, R. Wang, Dr. K. Yang, J. Yu, Y. Shi, Dr. Y. Wang, Prof. X. Guo
Department of Materials Science and Engineering and The Shenzhen Key Laboratory for Printed Organic Electronics
Southern University of Science and Technology (SUSTech)
No. 1088, Xueyuan Road, Shenzhen, Guangdong 518055, China
E-mail: guoxg@sustc.edu.cn

Dr. H. Sun
Institute of Polymer Optoelectronic Materials and Devices
State Key Laboratory of Luminescent Materials and Devices
South China University of Technology
Guangzhou, Guangdong 510640, China

C. W. Koh, Prof. H. Y. Woo
Research Institute for Natural Sciences
Department of Chemistry
Korea University
Seoul 136-713, South Korea

The ORCID identification number(s) for the author(s) of this article can be found under https://doi.org/10.1002/adma.201807220.

DOI: 10.1002/adma.201807220

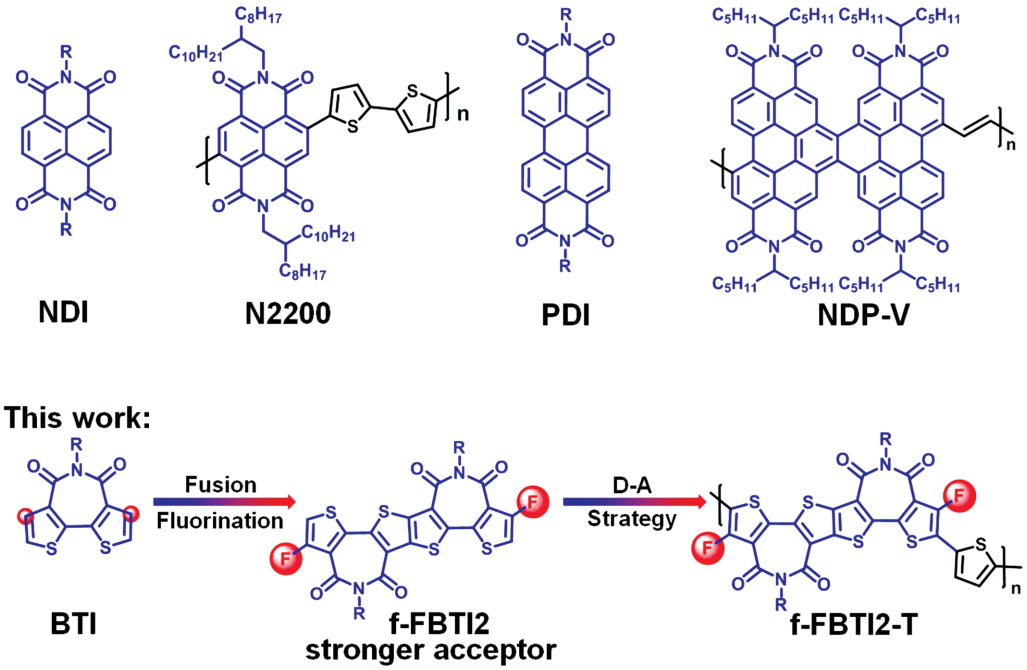

Figure 1. (Top) Chemical structures of NDI and PDI as well as their corresponding best-performing n-type polymers for all-PSCs with PCEs > 8%. (Bottom) Synergistic strategy via ring fusion and fluorination for the molecular design of f-FBTI2 and the resulting polymer f-FBTI2-T (this work).

family of imide-functionalized arenes.[4b,c,8] Unlike well-known NDIs and PDIs, the thiophene-based cores in BTIn can greatly reduce steric hindrance with neighboring arenes when incorporated into polymer semiconductors. However, compared to naphthalene and perylene, thiophene is more electron-rich, which can partially offset the electron-withdrawing effect of imide functionality, leading to decreased electron affinities of BTIn versus those of NDI or PDI. Therefore, functionalizing BTIn with other electron-withdrawing atoms or groups should yield stronger electron acceptors and address the steric hindrance issue associated with NDI and PDI.

In addition to the ring fusion, the strategy of fluorination has shown remarkable success for improving device performance of organic and polymeric semiconductors attributed to the small atomic size and high electronegativity of fluorine (F) atom.[9] In spite of such great success of fluorination strategy, it should be pointed out that the fluorinated polymers reported in literature are mainly based on commercially available fluorinated arenes, such as fluorinated thiophenes, fluorinated benzothiadiazoles, and fluorinated benzotriazoles, or the fluorinated arenes with limited synthetic challenges. The electron-withdrawing capability of such fluorinated arenes typically is not sufficiently strong, hence the fluorinated polymers mainly function as p-type polymer donors in PSCs.[1e,3a,b,9] Functionalizing highly electron-deficient arenes with F atoms is well desired in terms of optimizing electronic structures and developing n-type polymers, but is also very challenging due to the synthetic barriers and the companying steric hindrance. Herein we designed and overcome the barriers to successfully synthesize a novel electron-deficient building block, di(fluorothienyl) thienothiophene diimide (f-FBTI2, Figure 1). f-FBTI2 features two F atoms on the thiophene β-positions, which are expected to yield a stronger acceptor building block than the previously reported f-BTI2.[4c] Density functional theory (DFT)-based calculations revealed that f-FBTI2 has lower-lying lowest unoccupied molecular orbital (LUMO)/highest occupied molecular orbital (HOMO) level than f-BTI2 and s-BTI2 generated only by BTI ring fusion or dimerization strategy, respectively (Figure S1, Supporting Information),[4c] which should lead to f-FBTI2-based polymers with improved n-type characteristics. To promote intramolecular charge transfer (ICT) characteristics and maximize n-type performance, f-FBTI2 was copolymerized with donor counit with minimal thiophene number, i.e., monothiophene here, to afford a new donor–acceptor (D–A) type copolymer f-FBTI2-T (Figure 1). To show the effect of fluorination on promoting all-PSC performance, a new nonfluorinated analog polymer f-BTI2-T (Figure 1) was also synthesized. As a result of the optimized polymer electronic property, f-FBTI2-T yielded excellent all-PSC performance with a PCE up to 8.1%, which is substantially higher than that (5.4%) of the solar cells based on the polymer analog f-BTI2-T. This efficiency is the highest value reported for all-PSCs except the well-studied NDI and PDI-based polymers,[3a,c,d] suggesting the high efficacy of fluorination of acceptor building block on improving all-PSC performance.

Directly introducing F atoms onto highly electron-deficient imide-functionalized arenes is challenging due to low chemical reactivity and accompanied steric hindrance. In this work, we devised a synthetic route by fluorinating thiophene first and then forming imide later (**Scheme 1**). The compound **1** was synthesized from commercial 2,3,4,5-tetrabromothiophene based on the Heeney's protocol, which successfully tackled the synthetic challenge to obtain the monofluorinated thiophene precursor.[10] The key unsymmetrical intermediate propyl 4-fluoro-2,5-bis(trimethylsilyl)thiophene-3-carboxylate

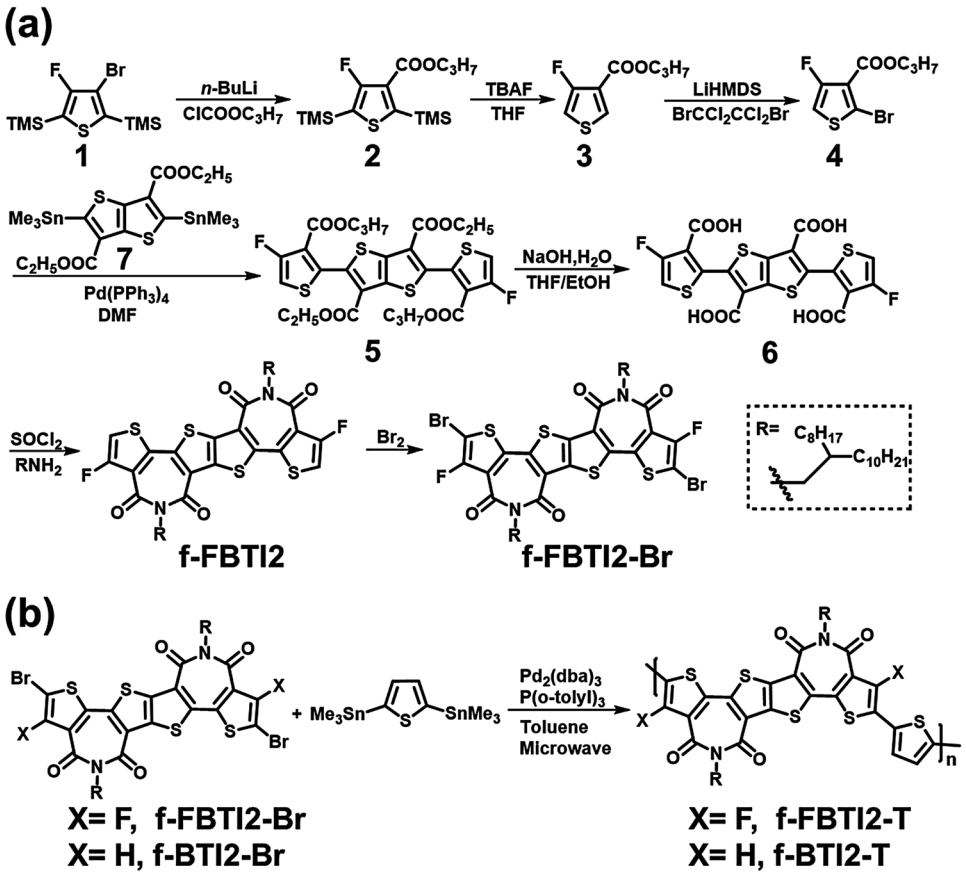

Scheme 1. Synthetic route to a) the new fluorinated imide-functionalized monomer f-FBTI2-Br and b) the corresponding polymer semiconductor f-FBTI2-T together with the nonfluorinated polymer analog f-BTI2-T.

2 was synthesized via the halogen-lithium exchange reaction, followed by the treatment with electrophilic propyl carbonochloridate. Compound **2** can be readily deprotected using tetra-*n*-butylammonium fluoride, affording propyl 4-fluorothiophene-3-carboxylate **3**, which can be successfully brominated with a high regioselectivity under the treatment of lithium hexamethyldisilazide (LiHMDS) and 1,2-dibromo-1,1,2,2-tetrachloroethane ($BrCCl_2CCl_2Br$) to yield the key product, propyl 2-bromo-4-fluorothiophene-3-carboxylate **4**.[11] Stille coupling **4** with compound **7**[4b] afforded tetracarboxylate **5**. The subsequent hydrolysis produced tetracarboxylic acid **6** in 90% yield, which was then converted to f-FBTI2 via a facile and efficient imidization method.[8b] The dibrominated monomer f-FBTI2-Br was readily attained from f-FBTI2 in a high yield of 92% by bromination under reflux. The new BTI-based polymer f-FBTI2-T was synthesized through the typical Stille coupling-based polycondensation between f-FBTI2-Br and 2,5-bis(trimethylstannyl) thiophene. A new nonfluorinated polymer analog f-BTI2-T was also synthesized for comparison. Both polymers had comparable number-average molecular weights (M_ns = 16 kDa) and exhibited good solubility in a range of organic solvents and high thermal stability (Table S1 and Figure S2a, Supporting Information). The differential scanning calorimetry (DSC) curves show no distinctive thermal transition (Figure S2b, Supporting Information). Such phenomena have also been observed in many ladder-type organic semiconductors,[2a,b,7] which likely suggest that the polymer melting point is greater than their decomposition temperature.

UV–vis absorption spectra of both polymers are shown in **Figure 2**a. Two absorption peaks were observed at ≈ 600 and 650 nm for the nonfluorinated f-FBTI2-T film, which are red-shifted by ≈20 or 40 nm relative to those of f-BTI2-T without F and the previously reported f-BTI2-FT in which two F atoms are on the electron-rich thiophene co-unit[4c] (Table S1, Supporting Information), respectively. It was also observed that both f-FBTI2-T and f-BTI2-T show greatly enhanced absorption coefficient than that of the benchmark n-type polymer N2200 (Figure S3, Supporting Information) contributed to their more planar polymer backbone, which reflects the advantages of our polymers and should benefit to photocurrent improvement in solar cells. Based on film absorption onsets, the calculated optical bandgap (E_g^{opt}) is 1.74 and 1.79 eV for f-FBTI2-T and f-BTI2-T, respectively, which fluorinating acceptor unit led to a narrower E_g^{opt} (1.74 eV) for polymer f-FBTI2-T compared to that (1.84 eV) of the analog f-BTI2-FT with F on the donor counit[4c] (Table S1, Supporting Information). The decreased E_g^{opt} of f-FBTI2-T can be attributed to a higher ICT character enabled by the more electron-deficient f-FBTI after fluorination.[12] The results demonstrate that fluorinating acceptor leads to "stronger acceptor," which is well desired in terms of decreasing E_g^{opt} and promoting n-type characteristics. Additionally, from solution to film, both polymers show nearly

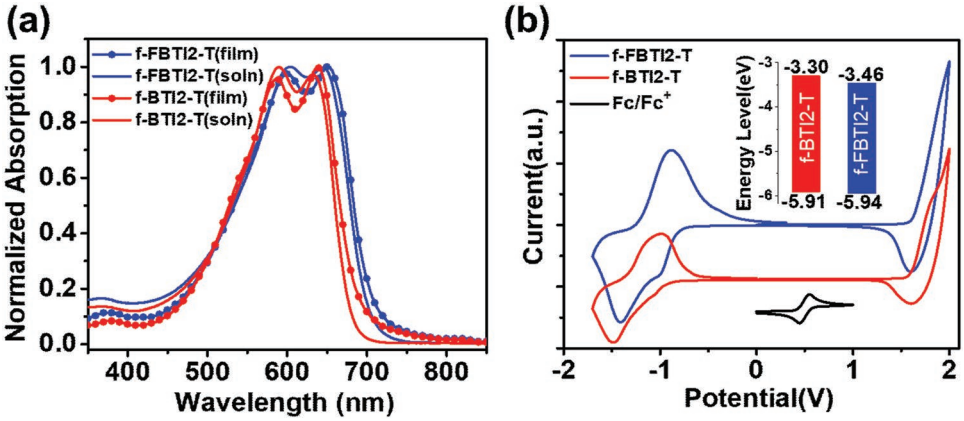

Figure 2. a) Solution and film UV–vis absorption spectra of f-FBTI2-T and f-BTI2-T. b) Cyclic voltammograms of f-FBTI2-T and f-BTI2-T, inset shows the corresponding energy diagram.

identical absorption spectra (Figure 2a), and the absorption was even unchanged when the solution was heated to 100 °C (Figure S4, Supporting Information), indicative of strong aggregation characteristics of both polymers in solution even at high temperature. Based on the cyclic voltammetry measurements, the LUMO/HOMO levels were determined to be ≈−3.46/−5.94 and −3.30/−5.91 eV for f-FBTI2-T and f-BTI2-T, respectively (Figure 2b). Hence the LUMO of f-FBTI2-T was lowered by a sizable margin (0.16 eV) after fluorination of f-BTI2-T and slightly lower than that (-3.43 eV) of f-BTI2-FT with F atoms on thiophene moiety, which in combination with the smaller E_g^{opt} of f-FBTI2-T reflects the advantages of fluorination of acceptor (versus fluorination of donor). DFT calculations confirmed the lower-positioned LUMO level of f-FBTI2-T by 0.1 and 0.06 eV than that of f-BTI2-T and f-BTI2-FT (Table S1, Supporting Information), respectively, which is conducive to improving the electron-accepting ability of polymer f-FBTI2-T. These optoelectronic properties substantially benefit to a higher photovoltaic efficiency as revealed in the following.

All-PSCs were fabricated to investigate the polymer photovoltaic performance using a conventional device structure of indium tin oxide (ITO)/poly(3,4-ethylenedioxythiophene): poly(styrenesulfonate) (PEDOT:PSS)/active layer/LiF/Al. The well-known PTB7-Th was chosen as the polymer donor due to its superior performance in various types of OSCs and its complementary absorption with the two acceptor polymers (Figure S5, Supporting Information).[13] Therefore, the blend films cover a broad spectral range from 300 to 750 nm, which is a desirable feature for enhanced light harvesting and thus increases of photocurrent generation in all-PSCs. The active layer was spin coated from a chlorobenzene solution having varied PTB7-Th:f-FBTI2-T (or f-BTI2-T) weight ratio between 1.5:1 and 1:2.5. As shown in **Table 1** and Tables S2–S21 in the Supporting Information, the optimized conditions involved a PTB7-Th:polymer acceptor ratio of 1:2.25 (or 1:2) without using any solvent additive. Under such condition, a relatively large acceptor polymer loading in active layer yielded a higher J_{sc} value (Table S2, Supporting Information), which is likely attributed to their higher absorption coefficient in pristine film compared to that of the donor polymer (Figure S5, Supporting Information).[1e,3b,g] The current density–voltage (J–V) curves and the external quantum efficiency (EQE) spectra of the all-PSCs obtained under AM1.5G illumination at 100 mW cm^{-2} are depicted in **Figure 3**.

The PTB7-Th:f-BTI2-T all-PSCs exhibited a promising PCE of 5.40% with a remarkable open-circuit voltage (V_{oc}) of 1.13 V (Table 1). This large V_{oc} stems from the high-lying LUMO of f-BTI2-T, corresponding to an energy loss (E_{loss}) of only 0.45 eV as calculated based on $E_{loss} = E_g - eV_{oc}$. Notably, E_{loss} is one of the most important parameters determining the performance of OSCs; however, a variety of methods used to determine E_g make it hard for consistent comparison of E_{loss} among different material systems and solar cell devices.[14] In our case, we use the most practiced one to determine E_g in OSC community, where E_g is the optical gap of the material (donor or acceptor) with the smaller value in the blend, here PTB7-Th. Hence the E_g was extracted from the absorption onset of PTB7-Th and was determined to be 1.58 eV, which is consistent with the previous values reported by Zhan and co-workers and Liu and co-workers.[15] In addition, we also determined the E_g based on three other methods for comparison and the corresponding E_{loss}s are included in Figure S6 in the Supporting Information.

Table 1. Photovoltaic performance parameters of all-PSCs based on PTB7-Th:f-FBTI2-T (or f-BTI2-T) blend films.

Polymer acceptor[a,b]	V_{oc} [V]	J_{sc} [mA cm^{-2}]	FF [%]	PCE$_{avg}$ [%]	PCE$_{max}$ [%]	E_{loss} [eV]
f-FBTI2-T	1.05 (1.04 ± 0.01)	13.60 (13.45 ± 0.15)	56.5 (54.9 ± 1.06)	8.0 ± 0.1	8.1	0.53
f-BTI2-T	1.13 (1.11 ± 0.02)	9.68 (9.48 ± 0.20)	49.2 (47.7 ± 1.50)	5.3 ± 0.1	5.4	0.45

[a]The highest PCEs and average PCEs with standard deviations in parentheses are calculated from 15 devices at least.; [b]More detailed performance statistics can be found in Tables S2–S21 in the Supporting Information.

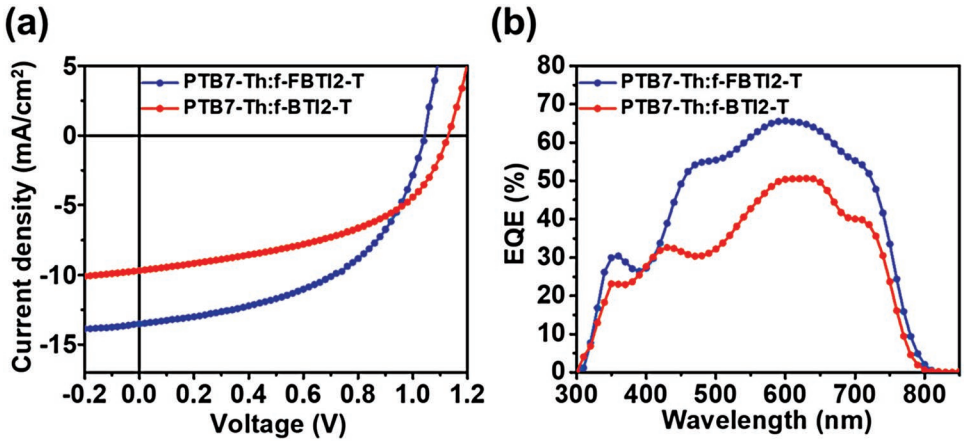

Figure 3. a) *J–V* curves and b) EQE spectra of the optimized all-PSCs containing PTB7-Th:f-FBTI2-T (or PTB7-Th:f-BTI2-T) active layer.

In OSCs, the LUMO offset between the donor material and the acceptor material makes one of the major contributors to the overall E_{loss} in devices.[16] The f-FBTI2-T showed a lower-lying LUMO than f-BTI2-T, which resulted in a larger LUMO offset between PTB7-Th and f-FBTI2-T than that between PTB7-Th and f-BTI2-T. Hence, the f-FBTI2-T-based all-PSCs yielded a slightly larger E_{loss} of 0.53 eV than the nonfluorinated f-BTI2-T-based all-PSCs. The 0.45 eV E_{loss} in the f-BTI2-T-based cells is the smallest value reported for all-PSCs having a PCE > 5%, indicating a great room for further PCE enhancements.[15b,16b]

As expected, benefiting from the effect of fluorination, the PTB7-Th:f-FBTI2-T all-PSCs yielded a remarkable PCE over 8.1% with a very large V_{oc} of 1.05 V. Note that the PCE is greatly larger than that (6.8%) of the previously reported f-BTI2-FT-based all-PSCs (Table S23, Supporting Information). To the best of our knowledge, this PCE is among the highest values reported till today in all-PSCs.[1e,3d,17] Very recently PCEs greater than 11% were reported from all-polymer solar cells, such great progress was achieved based on the well-known n-type polymer N2200. The homojunction all-polymer tandem solar cells not only achieved a PCE of 11.2% but also enabled good device stability with PCE retaining 93% of the initial value after 1000 h aging at 80 °C.[17b] The high-performance N2200-based all-PSCs can also be realized by using green solvent system,[17c] which shows a great promise towards real application and commercialization. Greatly differing from these excellent works, which are mainly focusing on device engineering and materials processing using known materials.[17b,c] Our work is materials oriented, reporting the design and synthesis of a new high-performance n-type polymer based on a novel building block f-FBTI2. Such new electron-deficient building block and n-type polymer are highly pursed in the field of all-polymer solar cells.

Notably, although solvent additives have been widely used to further improve solar cell performance, they often lead to decreased morphology and device stability. Achieving optimal photovoltaic performance without any solvent additives greatly simplifies device fabrication and also provides benefits for manufacturing large-scale devices in a high-throughput fashion.[18] Compared to the f-BTI2-T-based all-PSCs, the higher PCE achieved in the f-FBTI2-T-based cells resulted from the increased short-circuit current density (J_{sc}) and fill factor (FF). The higher J_{sc} likely arises from the improved exciton dissociation and charge transport enabled by the lower-lying polymer LUMO and more favorable blend morphology (vide infra) after fluorination.

The EQE curve of f-FBTI2-T shows broad photoresponses from 300 to 800 nm, with the highest EQE value of 66% recorded at ≈600 nm (Figure 3) compared to that of f-BTI2-T (51%) and f-BTI2-FT-based solar cells (56%), contributing to a much increased J_{sc} (13.6 mA cm^{-2}) achieved by f-FBTI2-T-based all-PSCs (Table S23, Supporting Information). The J_{sc} values integrated from the EQE curves are nearly identical with the ones obtained from the *J–V* curves, validating the reliability of the results. The increased J_{sc} and FF of the f-FBTI2-T cells is also attributed to the higher and more balanced charge carrier mobilities as revealed by the measurements using the space-charge-limited current (SCLC) method (Figure S7, Supporting Information). The SCLC hole ($\mu_{h,sclc}$) and electron ($\mu_{e,sclc}$) mobilities were found to be 5.4×10^{-5} and 4.0×10^{-6} cm^2 V^{-1} s^{-1} for PTB7-Th:f-BTI2-T blend, respectively, which were increased to 1.0×10^{-4} and 1.6×10^{-5} cm^2 V^{-1} s^{-1} for PTB7-Th:f-FBTI2-T blend. The greatly increased (up to approximately five times) mobilities of the PTB7-Th:f-FBTI2-T blend could reduce space charge accumulation and recombination, thus yielding the larger J_{sc} and FF.

Film morphologies and microstructures play critical roles on determining device performance, which were investigated by atomic force microscopy (AFM) and transmission electron microscopy (TEM) (**Figure 4**a,b). The surface root-mean-square roughnesses for the PTB7-Th:f-BTI2-T and PTB7-Th:f-FBTI2-T blend films were 1.61 and 0.55 nm, respectively, implying that the surface of the PTB7-Th:f-FBTI2-T blend was considerably smoother than that of the PTB7-Th:f-BTI2-T blend, likely attributed to better mixing between PTB7-Th and f-FBTI2-T, which is beneficial for the charge generation and extraction to electrodes. As shown in AFM phase images, the PTB7-Th:f-BTI2-T blend film exhibits a fibril-like nanostructure with coarse phase morphology, while the PTB7-Th:f-FBTI2-T blend film shows a phase separation at finer nanoscale with a collapsed fibril structure, indicating forming a better miscibility between PTB7-Th and f-FBTI2-T. The AFM morphological difference between the two blend films is consistent with the TEM images. The

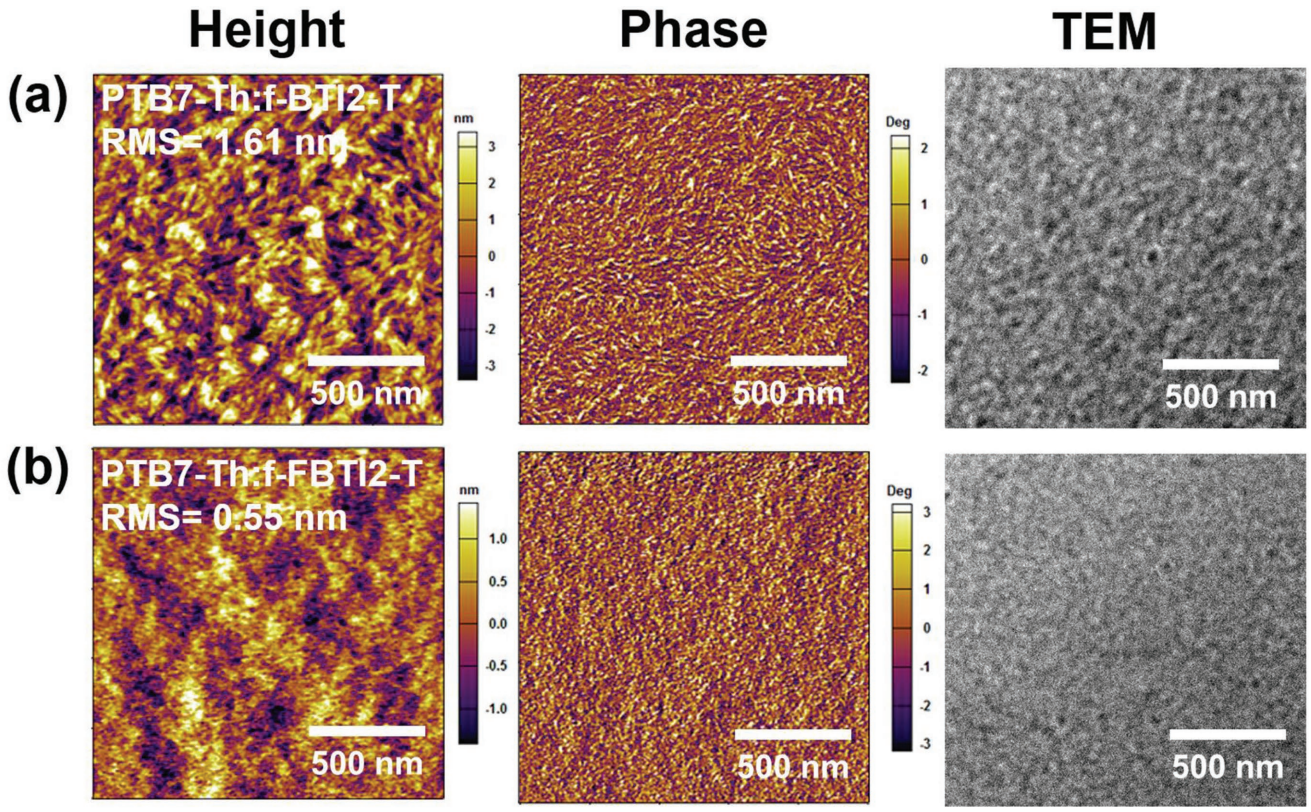

Figure 4. AFM height, phase images and TEM images of a) PTB7-Th:f-BTI2-T blend film and b) PTB7-Th:f-FBTI2-T blend film.

PTB7-Th:f-BTI2-T blend exhibited larger domains, whereas the PTB7-Th:f-FBTI2-T blend featured smaller domains with better domain connectivity. The smaller and better interconnected domains in PTB7-Th:f-FBTI2-T blend film facilitated the efficient exciton dissociation and charge collection, thus yielding the increased J_{sc} (13.60 mA cm^{-2}) than that (9.6 mA cm^{-2}) of nonfluorinated analog. Such improved film morphology of PTB7-Th:f-FBTI2-T blend is likely attributed to the improved crystallinity compatibility between PTB7-Th and f-FBTI2-T.[19] Photoluminescence (PL) quenching measurements were performed to further assess exciton dissociation in the blend films. As depicted in Figure S9 in the Supporting Information, the fluorescence of polymer donor PTB7-Th was effectively quenched by mixing it with two polymer acceptors f-FBTI2-T or f-BTI2-T. The PL quenching efficiency in the PTB7-Th:f-FBTI2-T blend reached 95%, while that in the PTB7-Th:f-BTI2-T blend was only 80%. These results indicate that the photoinduced charge transfer is far more efficient in the PTB7-Th:f-FBTI2-T blend film.

To further understand the improvements of J_{sc} and FF after fluorination, the polymer packing structures of the neat and blend films were studied using grazing incidence X-ray diffraction (GIXD). The 2D GIXD patterns of f-BTI2-T and f-FBTI2-T neat films are shown in **Figure 5**a,c, together with corresponding 1D line-cut profiles (Figure 5e,f). The f-BTI2-T film exhibited an edge-on predominant orientation with a (010) π–π stacking peak (d-spacing of ≈3.6 Å) in the in-plane (IP) direction and pronounced interlamellar scatterings up to (400) in the out-of-plane (OOP) direction (d-spacing of 2.6 nm) (Table S24, Supporting Information). In contrast, resulting from the effect of fluorination on crystallite orientation,[9a] the neat f-FBTI2-T film exhibited a face-on dominating bimodal orientation showing a hump-shaped (100) lamellar diffraction and a (010) π–π stacking peak (d-spacing of 3.6–3.7 Å) in the OOP direction. By mixed with PTB7-Th, both blend films showed enhanced face-on orientation (Figure 5b,d). Especially, a clear increased face-on packing was observed in the PTB7-Th:f-FBTI2-T blend film with a significantly intensified π–π stacking (010) peak in the OOP direction. A higher crystal coherence length (CCL) was also calculated for PTB7-Th:f-FBTI2-T film (20.9 Å) compared to f-BTI2-T:PTB7-Th film (17.8 Å) from the full width at half maximum of the OOP (010) peak (Table S25, Supporting Information). Hence, fluorination promoted face-on orientation of polymer chains and also led to increased CCL value. Both structural features are conducive to vertical charge transport, as evidenced by the SCLC mobility measurements, which reduced bimolecular recombination in all-PSCs and thus led to higher J_{sc} and FF in the f-FBTI2-T-based device.[20]

In summary, we have developed a novel imide type electron-deficient building block f-FBTI2 featuring a ladder-type backbone functionalized with electron-withdrawing F atoms. The synthetic barriers associated with the development of highly electron-deficient fluorinated imide were successfully overcome, which can enlarge imide-functionalized arenes, well desired building blocks in organic electronics. The synergistic strategy combining ring fusion and fluorination enables

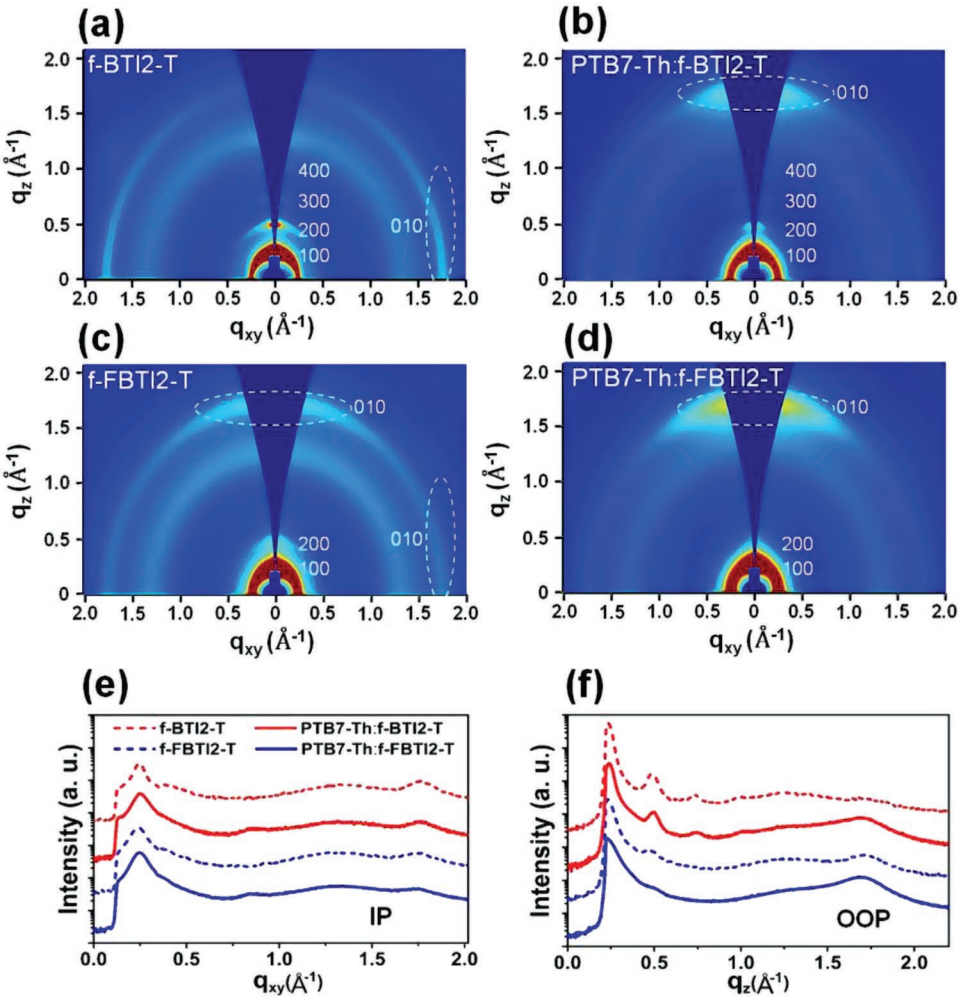

Figure 5. 2D GIXD images of the neat and blend polymer films: a) f-BTI2-T, b) PTB7-Th:f-BTI2-T, c) f-FBTI2-T, and d) PTB7-Th:f-FBTI2-T. Line-cut profiles in the e) IP and f) OOP directions.

f-FBTI2-based polymer with an extended π-conjugation, reduced bandgap, and lower-lying LUMO energy level versus the polymer analog without F atoms or with F-functionalization on the electron-rich donor moiety. These optoelectronic properties reflect the distinctive advantages of fluorination of electron-deficient acceptors, yielding "stronger acceptors," which are highly pursued for enabling n-type polymer semiconductors. Benefitting from these properties, the all-PSCs using f-FBTI2-T as the n-type polymer acceptor exhibited an extraordinary PCE of 8.1% without using any solvent additive or thermal treatment, which is the highest value reported to date for all-PSCs except the well-known NDI and PDI-based n-type polymers. In addition, the f-FBTI2-T-based all-PSCs showed a remarkable V_{oc} of 1.05 V with a minimal E_{loss} of 0.53 eV, indicating a great potential for further device performance improvement. The results demonstrate that fluorination of imide-functionalized arenes is a very effective approach to develop new electron-deficient building blocks with optimized geometry and optoelectronic property for high-performance n-type polymer acceptors. The emergence of f-FBTI2 will greatly change the scenario in terms of developing n-type polymer semiconductors for high-performance all-PSCs, which are dominated by NDI and PDI-based polymers till today.

Supporting Information

Supporting Information is available from the Wiley Online Library or from the author.

Acknowledgements

H.S. and Y.T. contributed equally to this work. The authors thank National Natural Science Foundation of China (51573076 and 21801124), Shenzhen Basic Research Fund (JCYJ20170817105905899), Shenzhen Peacock Plan Project (KQTD20140630110339343), and the Shenzhen Key Lab funding (ZDSYS201505291525382). H.Y.W. is grateful to the financial support from the National Research Foundation of Korea (2016M1A2A2940911 and 2015M1A2A2057506).

Conflict of Interest

The authors declare no conflict of interest.

Keywords

all-polymer solar cells, fluorination, imide-functionalized arene, n-type polymer, organic electronics

Received: November 7, 2018
Revised: January 24, 2019
Published online: February 15, 2019

[1] a) H. Kang, W. Lee, J. Oh, T. Kim, C. Lee, B. J. Kim, *Acc. Chem. Res.* **2016**, *49*, 2424; b) N. J. Zhou, A. Facchetti, *Mater. Today* **2018**, *21*, 377; c) T. Kim, J. H. Kim, T. E. Kang, C. Lee, H. Kang, M. Shin, C. Wang, B. Ma, U. Jeong, T. S. Kim, B. J. Kim, *Nat. Commun.* **2015**, *6*, 8547; d) Y. Diao, Y. Zhou, T. Kurosawa, L. Shaw, C. Wang, S. Park, Y. Guo, J. A. Reinspach, K. Gu, X. Gu, B. C. Tee, C. Pang, H. Yan, D. Zhao, M. F. Toney, S. C. Mannsfeld, Z. Bao, *Nat. Commun.* **2015**, *6*, 7955; e) X. Liu, C. Zhang, C. Duan, M. Li, Z. Hu, J. Wang, F. Liu, N. Li, C. J. Brabec, R. A. J. Janssen, G. C. Bazan, F. Huang, Y. Cao, *J. Am. Chem. Soc.* **2018**, *140*, 8934; f) S. Chen, S. Jung, H. J. Cho, N. H. Kim, S. Jung, J. Xu, J. Oh, Y. Cho, H. Kim, B. Lee, Y. An, C. Zhang, M. Xiao, H. Ki, Z. G. Zhang, J. Y. Kim, Y. Li, H. Park, C. Yang, *Angew. Chem., Int. Ed.* **2018**, *57*, 13277; g) J. Yang, B. Xiao, A. Tang, J. Li, X. Wang, E. Zhou, *Adv. Mater.* **2018**, https://doi.org/10.1002/adma.201804699.

[2] a) C. Yan, S. Barlow, Z. Wang, H. Yan, A. K.-Y. Jen, S. R. Marder, X. Zhan, *Nat. Rev. Mater.* **2018**, *3*, 18003; b) J. Zhang, H. S. Tan, X. Guo, A. Facchetti, H. Yan, *Nat. Energy* **2018**, *3*, 720; c) J. Zhao, Y. Li, G. Yang, K. Jiang, H. Lin, H. Ade, W. Ma, H. Yan, *Nat. Energy* **2016**, *1*, 15027.

[3] a) L. Gao, Z. G. Zhang, L. Xue, J. Min, J. Zhang, Z. Wei, Y. Li, *Adv. Mater.* **2016**, *28*, 1884; b) B. Fan, L. Ying, Z. Wang, B. He, X. F. Jiang, F. Huang, Y. Cao, *Energy Environ. Sci.* **2017**, *10*, 1243; c) B. Fan, L. Ying, P. Zhu, F. Pan, F. Liu, J. Chen, F. Huang, Y. Cao, *Adv. Mater.* **2017**, *29*, 1703906; d) Y. Guo, Y. Li, O. Awartani, H. Han, J. Zhao, H. Ade, H. Yan, D. Zhao, *Adv. Mater.* **2017**, *29*, 1700309; e) Z. G. Zhang, Y. Yang, J. Yao, L. Xue, S. Chen, X. Li, W. Morrison, C. Yang, Y. Li, *Angew. Chem., Int. Ed.* **2017**, *56*, 13503; f) D. Chen, J. Yao, L. Chen, J. Yin, R. Lv, B. Huang, S. Liu, Z. G. Zhang, C. Yang, Y. Chen, Y. Li, *Angew. Chem., Int. Ed.* **2018**, *57*, 4580; g) N. B. Kolhe, H. Lee, D. Kuzuhara, N. Yoshimoto, T. Koganezawa, S. A. Jenekhe, *Chem. Mater.* **2018**, *30*, 6540.

[4] a) X. Guo, A. Facchetti, T. J. Marks, *Chem. Rev.* **2014**, *114*, 8943; b) Y. Wang, H. Guo, S. Ling, I. Arrechea-Marcos, Y. Wang, J. T. Lopez Navarrete, R. Ponce Ortiz, X. Guo, *Angew. Chem., Int. Ed.* **2017**, *56*, 9924; c) Y. Wang, Z. Yan, H. Guo, M. A. Uddin, S. Ling, X. Zhou, H. Su, J. Dai, H. Y. Woo, X. Guo, *Angew. Chem., Int. Ed.* **2017**, *56*, 15304; d) H. Xin, C. Ge, X. Jiao, X. Yang, K. Rundel, C. R. McNeill, X. Gao, *Angew. Chem., Int. Ed.* **2018**, *57*, 1322.

[5] F. Wurthner, C. R. Saha-Moller, B. Fimmel, S. Ogi, P. Leowanawat, D. Schmidt, *Chem. Rev.* **2016**, *116*, 962.

[6] a) J. A. Letizia, M. R. Salata, C. M. Tribout, A. Facchetti, M. A. Ratner, T. J. Marks, *J. Am. Chem. Soc.* **2008**, *130*, 9679; b) X. Guo, R. P. Ortiz, Y. Zheng, Y. Hu, Y.-Y. Noh, K.-J. Baeg, A. Facchetti, T. J. Marks, *J. Am. Chem. Soc.* **2011**, *133*, 1405.

[7] J. Chen, K. Yang, X. Zhou, X. Guo, *Chem. - Asian J.* **2018**, *13*, 2587.

[8] a) M. Saito, I. Osaka, Y. Suda, H. Yoshida, K. Takimiya, *Adv. Mater.* **2016**, *28*, 6921; b) Y. Wang, H. Guo, A. Harbuzaru, M. A. Uddin, I. Arrechea-Marcos, S. Ling, J. Yu, Y. Tang, H. Sun, J. T. Lopez Navarrete, R. P. Ortiz, H. Y. Woo, X. Guo, *J. Am. Chem. Soc.* **2018**, *140*, 6095.

[9] a) Q. Zhang, M. A. Kelly, N. Bauer, W. You, *Acc. Chem. Res.* **2017**, *50*, 2401; b) Y. Liang, D. Feng, Y. Wu, S. T. Tsai, G. Li, C. Ray, L. Yu, *J. Am. Chem. Soc.* **2009**, *131*, 7792; c) H. Zhou, L. Yang, A. C. Stuart, S. C. Price, S. Liu, W. You, *Angew. Chem., Int. Ed.* **2011**, *50*, 2995; d) A. C. Stuart, J. R. Tumbleston, H. Zhou, W. Li, S. Liu, H. Ade, W. You, *J. Am. Chem. Soc.* **2013**, *135*, 1806; e) S. C. Price, A. C. Stuart, L. Yang, H. Zhou, W. You, *J. Am. Chem. Soc.* **2011**, *133*, 4625.

[10] Z. Fei, P. Boufflet, S. Wood, J. Wade, J. Moriarty, E. Gann, E. L. Ratcliff, C. R. McNeill, H. Sirringhaus, J. S. Kim, M. Heeney, *J. Am. Chem. Soc.* **2015**, *137*, 6866.

[11] a) O. V. Serdyuk, V. T. Abaev, A. V. Butin, V. G. Nenajdenko, *Synthesis* **2011**, *2011*, 2505; b) H. Sun, J. Shi, Z. Zhang, S. Zhang, Z. Liang, S. Wan, Y. Cheng, H. Wang, *J. Org. Chem.* **2013**, *78*, 6271; c) P. Boufflet, Y. Han, Z. Fei, N. D. Treat, R. Li, D.-M. Smilgies, N. Stingelin, T. D. Anthopoulos, M. Heeney, *Adv. Funct. Mater.* **2015**, *25*, 7038; d) Q. Zhang, L. Yan, X. Jiao, Z. Peng, S. Liu, J. J. Rech, E. Klump, H. Ade, F. So, W. You, *Chem. Mater.* **2017**, *29*, 5990.

[12] J. M. Szarko, B. S. Rolczynski, S. J. Lou, T. Xu, J. Strzalka, T. J. Marks, L. P. Yu, L. X. Chen, *Adv. Funct. Mater.* **2014**, *24*, 10.

[13] a) Y. Liang, L. Yu, *Acc. Chem. Res.* **2010**, *43*, 1227; b) L. Ye, S. Zhang, L. Huo, M. Zhang, J. Hou, *Acc. Chem. Res.* **2014**, *47*, 1595.

[14] a) Y. Wang, D. Qian, Y. Cui, H. Zhang, J. Hou, K. Vandewal, T. Kirchartz, F. Gao, *Adv. Energy Mater.* **2018**, *8*, 1801352; b) V. C. Nikolis, J. Benduhn, F. Holzmueller, F. Piersimoni, M. Lau, O. Zeika, D. Neher, C. Koerner, D. Spoltore, K. Vandewal, *Adv. Energy Mater.* **2017**, *7*, 1700855.

[15] a) Y. Lin, J. Wang, Z.-G. Zhang, H. Bai, Y. Li, D. Zhu, X. Zhan, *Adv. Mater.* **2015**, *27*, 1170; b) X. Long, Z. Ding, C. Dou, J. Zhang, J. Liu, L. Wang, *Adv. Mater.* **2016**, *28*, 6504.

[16] a) D. Qian, Z. Zheng, H. Yao, W. Tress, T. R. Hopper, S. Chen, S. Li, J. Liu, S. Chen, J. Zhang, X. K. Liu, B. Gao, L. Ouyang, Y. Jin, G. Pozina, I. A. Buyanova, W. M. Chen, O. Inganas, V. Coropceanu, J. L. Bredas, H. Yan, J. Hou, F. Zhang, A. A. Bakulin, F. Gao, *Nat. Mater.* **2018**, *17*, 703; b) J. Liu, S. Chen, D. Qian, B. Gautam, G. Yang, J. Zhao, J. Bergqvist, F. Zhang, W. Ma, H. Ade, O. Inganäs, K. Gundogdu, F. Gao, H. Yan, *Nat. Energy* **2016**, *1*, 16089.

[17] a) S. Liu, Y. Firdaus, S. Thomas, Z. Kan, F. Cruciani, S. Lopatin, J. L. Bredas, P. M. Beaujuge, *Angew. Chem., Int. Ed.* **2018**, *57*, 531; b) K. Zhang, R. Xia, B. Fan, X. Liu, Z. Wang, S. Dong, H. L. Yip, L. Ying, F. Huang, Y. Cao, *Adv. Mater.* **2018**, *30*, 1803166; c) Z. Li, L. Ying, P. Zhu, W. Zhong, N. Li, F. Liu, F. Huang, Y. Cao, *Energy Environ. Sci.* **2019**, *12*, 157.

[18] Y. Huang, E. J. Kramer, A. J. Heeger, G. C. Bazan, *Chem. Rev.* **2014**, *114*, 7006.

[19] Y. J. Hwang, T. Earmme, B. A. E. Courtright, F. N. Eberle, S. A. Jenekhe, *J. Am. Chem. Soc.* **2015**, *137*, 4424.

[20] J. R. Tumbleston, B. A. Collins, L. Yang, A. C. Stuart, E. Gann, W. Ma, W. You, H. Ade, *Nat. Photonics* **2014**, *8*, 385.